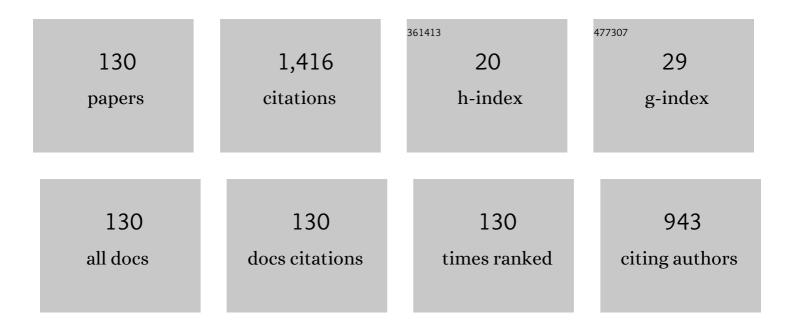
Ti-Ming Qu

List of Publications by Year in descending order

Source: https://exaly.com/author-pdf/7179155/publications.pdf Version: 2024-02-01



#	Article	IF	CITATIONS
1	Experimental investigation on the power and thrust characteristics of a wind turbine model subjected to surge and sway motions. Renewable Energy, 2022, 181, 1325-1337.	8.9	5
2	Screening current induced magnetic field and stress in ultra-high-field magnets using REBCO coated conductors. Superconductor Science and Technology, 2022, 35, 014003.	3.5	33
3	Wind tunnel study on the wake characteristics of a wind turbine model subjected to surge and sway motions. Journal of Renewable and Sustainable Energy, 2022, 14, .	2.0	3
4	Progress of ultra-high-field superconducting magnets in China. Superconductor Science and Technology, 2022, 35, 023001.	3.5	22
5	Effect of edge cracks on critical current degradation in REBCO tapes under tensile stress. , 2022, 1, 100007.		25
6	Thermal-Hydraulic Analysis on Quench Behavior of Indium-Tin Soldered REBCO Composite Conductor. IEEE Transactions on Applied Superconductivity, 2021, 31, 1-8.	1.7	1
7	Effect of Pitch Parameters on Aerodynamic Forces of a Straight-Bladed Vertical Axis Wind Turbine with Inclined Pitch Axes. Applied Sciences (Switzerland), 2021, 11, 1033.	2.5	2
8	Investigations on Quench Recovery Characteristics of High-Temperature Superconducting Coated Conductors for Superconducting Fault Current Limiters. Electronics (Switzerland), 2021, 10, 259.	3.1	6
9	A novel aluminum-carbon nanotubes nanocomposite with doubled strength and preserved electrical conductivity. Nano Research, 2021, 14, 2776-2782.	10.4	21
10	Numerical Modeling of AC Loss in HTS Coated Conductors and Roebel Cable Using T-A Formulation and Comparison With H Formulation. IEEE Access, 2021, 9, 49649-49659.	4.2	33
11	Progress in the Construction of a 20 T REBCO Insert Coil for High-Field All-Superconducting Magnets. IEEE Transactions on Applied Superconductivity, 2021, , 1-1.	1.7	1
12	Wrinkling surface of mono-layered thin film derived by using trifluoroacetate solution. Journal of Sol-Gel Science and Technology, 2021, 99, 13.	2.4	0
13	Screening-current-induced mechanical strains in REBCO insert coils. Superconductor Science and Technology, 2021, 34, 085012.	3.5	42
14	A CONTINUOUS VARIATION OF ROUGHNESS SCALING CHARACTERISTICS ACROSS FRACTAL AND NON-FRACTAL PROFILES. Fractals, 2021, 29, 2150109.	3.7	6
15	Design of a 20 T Class REBCO Insert in a 15 T Low Temperature Superconducting Magnet. Electronics (Switzerland), 2021, 10, 1741.	3.1	8
16	Development and Testing of a 300-kvar HTS Synchronous Condenser Prototype. IEEE Transactions on Applied Superconductivity, 2021, 31, 1-5.	1.7	7
17	Wind tunnel experiment on the influence of array configuration on the power performance of vertical axis wind turbines. Energy Conversion and Management, 2021, 241, 114299.	9.2	19
18	Critical current degradation and delamination crack observation of epoxy-coated REBCO superconducting tapes after thermal cycles in liquid nitrogen. Ceramics International, 2021, 47, 29824-29831.	4.8	7

#	Article	IF	CITATIONS
19	Improvement of bi-layered YBCO superconducting films by using Ag and Au interlayers. Ceramics International, 2020, 46, 3394-3399.	4.8	7
20	Numerical Investigation of the Coupling Effect in CORC Cable With Striated Strands. IEEE Transactions on Applied Superconductivity, 2020, 30, 1-5.	1.7	10
21	Simultaneously enhancing mechanical properties and electrical conductivity of aluminum by using graphene as the reinforcement. Materials Letters, 2020, 265, 127440.	2.6	24
22	Optimization of wind turbine yaw angles in a wind farm using a three-dimensional yawed wake model. Energy, 2020, 209, 118415.	8.8	47
23	Robustness of Surface Roughness against Low Number of Picture Elements and Its Benefit for Scaling Analysis. Coatings, 2020, 10, 776.	2.6	10
24	Experimental investigation of a novel vertical axis wind turbine with pitching and self-starting function. Energy Conversion and Management, 2020, 217, 113012.	9.2	29
25	General Design of a 300-Kvar HTS Synchronous Condenser Prototype. IEEE Transactions on Applied Superconductivity, 2020, 30, 1-5.	1.7	13
26	Screening current effect on the stress and strain distribution in REBCO high-field magnets: experimental verification and numerical analysis. Superconductor Science and Technology, 2020, 33, 05LT02.	3.5	52
27	Modeling and Performances of the Orthogonal Fluxgate Sensor Operated in Fundamental Mode. IEEE Transactions on Magnetics, 2020, 56, 1-7.	2.1	3
28	Design and Testing of a Gas-Helium Conduction Cooled REBCO Magnet for a 300Âkvar HTS Synchronous Condenser Prototype. IEEE Transactions on Applied Superconductivity, 2020, 30, 1-5.	1.7	11
29	Comparison of Different Driving Modes for the Wind Turbine Wake in Wind Tunnels. Energies, 2020, 13, 1915.	3.1	9
30	Magnetization and screening current in an 800 MHz (18.8 T) REBCO nuclear magnetic resonance insert magnet: experimental results and numerical analysis. Superconductor Science and Technology, 2019, 32, 105007.	3.5	55
31	A novel REBCO conductor design to reduce screening-current field in REBCO magnets. Physica Scripta, 2019, 94, 105803.	2.5	11
32	Open Magnetic Shielding by Superconducting Technology. IEEE Transactions on Applied Superconductivity, 2019, 29, 1-4.	1.7	2
33	Effective Measuring Position of Hall Probe and <inline-formula> <tex-math notation="LaTeX">\$j_mathrm{c}\$ </tex-math </inline-formula> Characterization of Rectangular HTS Thin Films. IEEE Transactions on Applied Superconductivity, 2019, 29, 1-5.	1.7	1
34	Experimental and Numerical Study on the Magnetization Process of Roebel Cable Segments. IEEE Transactions on Applied Superconductivity, 2019, 29, 1-5.	1.7	7
35	Influences of planarization modification and morphological filtering by AFM probe-tip on the evaluation accuracy of fractal dimension. Surface and Coatings Technology, 2019, 363, 436-441.	4.8	9
36	Biaxially textured (Bi, Pb)2Sr2Ca2Cu3O x thin films on LaAlO3 substrates fabricated via the chemical solution deposition method. Superconductor Science and Technology, 2019, 32, 045006.	3.5	2

#	Article	IF	CITATIONS
37	Inductance of Low-Frequency Small-Scale High-Temperature Superconducting Coils. IEEE Transactions on Applied Superconductivity, 2019, 29, 1-4.	1.7	13
38	Characterization of <i>I</i> _c Degradation in Bent YBCO Tapes. IEEE Transactions on Applied Superconductivity, 2019, 29, 1-5.	1.7	8
39	Scaling analysis of current influence on Hastelloy surface roughness in electro-polishing process. Rare Metals, 2019, 38, 142-150.	7.1	2
40	Investigations on the lead acetate addition in precursor solutions for YBCO superconducting film deposition. Surface and Coatings Technology, 2019, 358, 1017-1021.	4.8	4
41	Critical current survival in the YBCO superconducting layer of a delaminated coated conductor. Superconductor Science and Technology, 2018, 31, 045005.	3.5	11
42	Influence of Dip-Coating Temperature Upon Film Thickness in Chemical Solution Deposition. IEEE Transactions on Applied Superconductivity, 2018, 28, 1-5.	1.7	8
43	Surface scaling analysis of textured MgO thin films fabricated by energetic particle self-assisted deposition. Applied Surface Science, 2018, 437, 287-293.	6.1	14
44	Design and Test of a Double Pancake Coil for SMES Application Wound by HTS Roebel Cable. IEEE Transactions on Applied Superconductivity, 2018, 28, 1-5.	1.7	8
45	Design Study of a 10-kW Fully Superconducting Synchronous Generator. IEEE Transactions on Applied Superconductivity, 2018, 28, 1-5.	1.7	8
46	Roughness scaling extraction method for fractal dimension evaluation based on a single morphological image. Applied Surface Science, 2018, 458, 489-494.	6.1	25
47	Design of a 30-K/4-kJ HTS Magnet Cryocooled With Solid Nitrogen. IEEE Transactions on Applied Superconductivity, 2018, 28, 1-6.	1.7	12
48	A persistent-mode 0.5 T solid-nitrogen-cooled MgB ₂ magnet for MRI. Superconductor Science and Technology, 2017, 30, 024011.	3.5	38
49	Stress Reduction and Storage Capacity Enhancement of the HTS-SMES Using Reinforcing Overbanding Structure. IEEE Transactions on Applied Superconductivity, 2017, 27, 1-5.	1.7	6
50	Observation and Analysis of Defects in Impregnated YBCO Racetrack Coil. IEEE Transactions on Applied Superconductivity, 2017, 27, 1-4.	1.7	1
51	Test of an 8.66-T REBCO Insert Coil With Overbanding Radial Build for a 1.3-GHz LTS/HTS NMR Magnet. IEEE Transactions on Applied Superconductivity, 2017, 27, 1-5.	1.7	38
52	A REBCO Persistent-Current Switch (PCS): Test Results and Switch Heater Performance. IEEE Transactions on Applied Superconductivity, 2017, 27, 1-5.	1.7	12
53	Numerical Study on AC Loss Characteristics of REBCO Armature Windings in a 15-kW Class Fully HTS Generator. IEEE Transactions on Applied Superconductivity, 2017, 27, 1-6.	1.7	15
54	Vortex shaking study of REBCO tape with consideration of anisotropic characteristics. Superconductor Science and Technology, 2017, 30, 094006.	3.5	16

#	Article	IF	CITATIONS
55	Experimental realization of open magnetic shielding. Applied Physics Letters, 2017, 110, .	3.3	14
56	Fabrication of Bi-2223 superconducting thick films via a non-vacuum method on silver foil substrates. Materials Express, 2016, 6, 430-436.	0.5	2
57	Thermal analysis for the HTS stator consisting of HTS armature windings and an iron core for a 2.5 kW HTS generator. Superconductor Science and Technology, 2016, 29, 054007.	3.5	20
58	Study of AC Loss and Temperature Distribution of a BSCCO Coil Cooled in Liquid Nitrogen or Using a Cryocooler. IEEE Transactions on Applied Superconductivity, 2016, 26, 1-5.	1.7	8
59	Design and Test of a Novel Thermal Insulated Torque Coupling for a 15-kW Fully HTS Synchronous Generator. IEEE Transactions on Applied Superconductivity, 2016, 26, 1-5.	1.7	7
60	Property Improvement of 600-nm-Thick YBCO Superconducting Films Fabricated Using a Pb-Modified MOD Method. IEEE Transactions on Applied Superconductivity, 2016, 26, 1-5.	1.7	10
61	Thermodynamics and Kinetics Analysis of MOD-YBCO Heat Treatment Process Using in situ Resistance Measurement Method. IEEE Transactions on Applied Superconductivity, 2016, 26, 1-5.	1.7	3
62	Persistent-current switch for pancake coils of rare earth-barium-copper-oxide high-temperature superconductor: Design and test results of a double-pancake coil operated in liquid nitrogen (77–65) Tj ETQo	ე0 0 £ 3gB1	/O se rlock 10
63	A Method to Fabricate Biaxially Textured MgO Buffer Layer for HTS Coated Conductor. IEEE Transactions on Applied Superconductivity, 2016, 26, 1-5.	1.7	3
64	Resputtering effect during MgO buffer layer deposition by magnetron sputtering for superconducting coated conductors. Journal of Vacuum Science and Technology A: Vacuum, Surfaces and Films, 2015, 33, .	2.1	11
65	Examination and Analysis of Critical Current Uniformity of Long HTS Tapes by the MCorder. IEEE Transactions on Applied Superconductivity, 2015, 25, 1-4.	1.7	5
66	Design and Optimization of Highâ€Temperature Superconducting Racetrack Magnet for the Rotor of a 100â€kW Generator. IEEE Transactions on Applied Superconductivity, 2015, 25, 1-5.	1.7	12
67	An Experimental Investigation of Critical Current and Current Distribution Behavior of Parallel Placed HTS Tapes. IEEE Transactions on Applied Superconductivity, 2015, 25, 1-5.	1.7	10
68	Enhancing Phase Purity of CSD Bi-2223 Thin Films Through Protected Sintering Method. IEEE Transactions on Applied Superconductivity, 2015, 25, 1-4.	1.7	1
69	Surface characterization of as-grown CeO ₂ cap layer morphology evolution and critical current density of post-deposited YBCO films. Materials Express, 2015, 5, 534-540.	0.5	6
70	Simulation of AC Loss in Small HTS Coils With Iron Core. IEEE Transactions on Applied Superconductivity, 2015, 25, 1-5.	1.7	21
71	Preparation of c-axis textured Bi-2212 thin films on silver substrates by using chemical solution deposition. Journal of Physics: Conference Series, 2014, 507, 012019.	0.4	1
72	A low-fluorine solution with a 2:1 F/Ba mole ratio for the fabrication of YBCO films. Superconductor Science and Technology, 2014, 27, 055006.	3.5	28

#	Article	IF	CITATIONS
73	Strain evolution and morphological transition of magnetron-sputtered CeO2 thin films induced by deposition parameters. Current Applied Physics, 2014, 14, 275-281.	2.4	4
74	Simulation of Current Profile and AC Loss of HTS Winding Wound by Parallel-Connected Tapes. IEEE Transactions on Applied Superconductivity, 2014, 24, 117-124.	1.7	2
75	Development and testing of a 2.5 kW synchronous generator with a high temperature superconducting stator and permanent magnet rotor. Superconductor Science and Technology, 2014, 27, 044026.	3.5	43
76	Critical current density improvement by intermediate deformation for the fabrication of Bi ₂ Sr ₂ Ca ₂ Cu ₃ O _{10+δ} /Ag round wires. Materials Express, 2014, 4, 105-114.	0.5	2
77	Loss measurement and analysis for the prototype generator with HTS stator and permanent magnet rotor. Physica C: Superconductivity and Its Applications, 2013, 494, 225-229.	1.2	7
78	AC Losses in HTS Tapes and Devices With Transport Current Solved Through the Resistivity-Adaption Algorithm. IEEE Transactions on Applied Superconductivity, 2013, 23, 8201708-8201708.	1.7	11
79	Investigation on the phase transformation of Bi-2223/Ag superconducting tapes during heating. Physica C: Superconductivity and Its Applications, 2013, 490, 43-48.	1.2	1
80	Simulation and Test for the Thermal Behaviour of a Prototype Synchronous Generator with HTS Armature Windings. Physics Procedia, 2013, 45, 257-260.	1.2	4
81	Surface morphology evolution of CeO2/YSZ (001) buffer layers fabricated via magnetron sputtering. Applied Surface Science, 2013, 284, 150-154.	6.1	16
82	Study on the oxygenation process during the heat treatment of TFA-MOD YBCO thin films by in situ resistance measurement. Physica C: Superconductivity and Its Applications, 2013, 494, 148-152.	1.2	9
83	A Review of the Ion Beam Assisted Deposition Researches towards Industrialization for the Second Generation High Temperature Superconducting Wire Fabrication. Materials Science Forum, 2013, 745-746, 225-232.	0.3	1
84	A rapid process of YBa ₂ Cu ₃ O _{7â^îî} thin film fabrication using trifluoroacetate metal–organic deposition with polyethylene glycol additive. Superconductor Science and Technology, 2013, 26, 055013.	3.5	15
85	Continuous critical current measurement of high-temperature superconductor tapes with magnetic substrates using magnetic-circuit method. Review of Scientific Instruments, 2013, 84, 105106.	1.3	6
86	A water-free metal organic deposition method for YBa2Cu3O7â~'δthin film fabrication. Superconductor Science and Technology, 2013, 26, 115010.	3.5	10
87	IN SITU MULTI-FIELDS INVESTIGATION ON INSTABILITY AND TRANSFORMATION LOCALIZATION OF MARTENSITIC PHASE TRANSFORMATION IN NiTi ALLOYS. Jinshu Xuebao/Acta Metallurgica Sinica, 2013, 49, 17.	0.3	2
88	Study on the High Temperature Pressure Charging Procedure of Bi-2223/Ag Superconducting Tapes. IEEE Transactions on Applied Superconductivity, 2011, 21, 2832-2835.	1.7	4
89	Study on the formation of the liquid phase during heating process of Bi-2223/Ag superconducting tapes at various oxygen partial pressure by using in situ resistance measurement. Physica C: Superconductivity and Its Applications, 2011, 471, 1093-1096.	1.2	5
90	Fabrication and characterization of Ni-clad Bi-2223/Ag superconducting tapes. Physica C: Superconductivity and Its Applications, 2011, 471, 1103-1106.	1.2	0

#	Article	IF	CITATIONS
91	Comparative study on the critical current performance of Bi-2223/Ag and YBCO wires in low magnetic fields at liquid nitrogen temperature. Physica C: Superconductivity and Its Applications, 2011, 471, 293-296.	1.2	24
92	Method and Apparatus for Continuous \$I_{m c}\$ Examination of HTS Tape Using Magnetic Circuit. IEEE Transactions on Applied Superconductivity, 2011, 21, 3413-3416.	1.7	17
93	The influence of electroplastic rolling on the mechanical deformation and phase evolution of Bi-2223/Ag tapes. Journal of Materials Science, 2010, 45, 3514-3519.	3.7	12
94	Experimental Study of Local Micro-forming for Bi-HTS. , 2010, , .		0
95	Contactless measurement of critical current of high temperature superconductor tape by magnetic circuit. Review of Scientific Instruments, 2010, 81, 085105.	1.3	13
96	The Design and Winding Method of a Conduction-Cooled 1.5 T Bi-2223 High Temperature Superconducting Magnet. IEEE Transactions on Applied Superconductivity, 2010, 20, 2002-2005.	1.7	3
97	Design of HTS Coil for Magnetic Driving Spacecraft. IEEE Transactions on Applied Superconductivity, 2010, 20, 997-1000.	1.7	3
98	Passive magnetic field cancellation device by multiple high-Tc superconducting coils. Review of Scientific Instruments, 2010, 81, 045101.	1.3	9
99	The Effect of Hot Isostatic Pressure on the Microstructure and Critical Current of Bi-2223/Ag Superconducting Tapes. IEEE Transactions on Applied Superconductivity, 2009, 19, 3045-3048.	1.7	4
100	Design and construction of the magnetic driving vehicle in a two-dimensional testbed. Superconductor Science and Technology, 2009, 22, 075011.	3.5	3
101	Investigation on drawing process of Bi-2223/Ag wires using racetrack-type dies: Simulation and experiments. Science in China Series D: Earth Sciences, 2009, 52, 2255-2262.	0.9	2
102	The Influence of Gas Flow Rate on the Growth of YBCO Films Prepared by TFA-MOD. IEEE Transactions on Applied Superconductivity, 2009, 19, 3123-3126.	1.7	3
103	Simulation of transport critical current of Bi2223/Ag tape with ferromagnetic shielding. Physica C: Superconductivity and Its Applications, 2008, 468, 1783-1786.	1.2	0
104	The study of a rotating method for fabricating Y1Ba2Cu3O7â^'x films by TFA-MOD. Physica C: Superconductivity and Its Applications, 2008, 468, 1869-1872.	1.2	5
105	Texture analysis of monofilamentary, Ag-sheathed (Pb,Bi)2Sr2Ca2Cu3Ox tapes by electron backscatter diffraction (EBSD). Physica C: Superconductivity and Its Applications, 2008, 468, 174-182.	1.2	9
106	The evolution of Bi-2223 phase and liquid phase during the first heat treatment in Bi-2223/Ag superconducting tapes. Physica C: Superconductivity and Its Applications, 2008, 468, 1767-1770.	1.2	2
107	Investigate on the application of elliptical drawing dies during the manufacturing process of Bi-2223/Ag superconducting tapes. Physica C: Superconductivity and Its Applications, 2008, 468, 1753-1755.	1.2	0
108	Increasing the density of the superconducting core by high pressure processing of Bi-2223/Ag tape. Superconductor Science and Technology, 2008, 21, 025019.	3.5	2

#	Article	IF	CITATIONS
109	Simulation of ferromagnetic shielding to the critical current of Bi2223/Ag tape under external fields. Superconductor Science and Technology, 2007, 20, 133-137.	3.5	14
110	Measurement and Calculation of Residual Magnetic Field in a Bi2223/Ag Magnet. IEEE Transactions on Applied Superconductivity, 2007, 17, 2394-2397.	1.7	44
111	The Influence of Tape Arrangements on the Critical Current of Bi-2223 Superconducting Current Leads. IEEE Transactions on Applied Superconductivity, 2007, 17, 2232-2235.	1.7	2
112	The influence of the first heat-treatment on the critical current density of (Bi,Pb)-2223/Ag superconducting tapes. Cryogenics, 2007, 47, 127-131.	1.7	2
113	The effect of high-pressure processing on unsealed Bi-2223/Ag tape. Physica C: Superconductivity and Its Applications, 2007, 463-465, 829-832.	1.2	1
114	The influence of post-annealing on the Pb3(Bi0.5Sr2.5)Ca2CuOy phase evolution and superconducting properties of (Bi,Pb)-2223/Ag tapes. Physica C: Superconductivity and Its Applications, 2007, 463-465, 833-836.	1.2	6
115	Fabrication and study of thin Bi-2223 round wires. Physica C: Superconductivity and Its Applications, 2007, 463-465, 837-840.	1.2	0
116	The effect of post-annealing on the critical current recovery of bending-deformed (Bi,Pb)-2223/Ag tapes. Physica C: Superconductivity and Its Applications, 2007, 463-465, 867-870.	1.2	1
117	The preparation and characterization of Bi-2212 film on Ag substrate by dip-coating method. Physica C: Superconductivity and Its Applications, 2006, 442, 134-138.	1.2	5
118	Phase evolution during post-annealing and its influence on critical currents of (Bi,Pb)-2223/Ag tapes. Physica C: Superconductivity and Its Applications, 2006, 444, 71-76.	1.2	27
119	Mechanical Properties of (Bi,Pb)-2223 Multifilament Tapes with Ag-Alloy Sheath. Chinese Physics Letters, 2006, 23, 964-966.	3.3	3
120	Effect of lead oxide compounds on microstructure and critical current density of (Bi,Pb)-2223/Ag tapes. Physica C: Superconductivity and Its Applications, 2005, 426-431, 1164-1169.	1.2	5
121	Voltage–current property of two HTS tapes connected by ordinary Sn–Pb solder. Physica C: Superconductivity and Its Applications, 2005, 426-431, 1385-1389.	1.2	15
122	V–I properties and n-value of degraded Bi-2223/Ag superconducting tapes. Physica C: Superconductivity and Its Applications, 2005, 426-431, 1159-1163.	1.2	3
123	Formation and growth studies of the (Bi,Pb)2Sr2Ca2Cu3O10 phase in Ag sheathed tapes. Journal of Materials Science, 2005, 40, 5721-5726.	3.7	12
124	Property of Joint Resistance of Bi2223 Multi-filamentary Tape by Using Sn-Pb Solder. , 2005, , 503-506.		0
125	Phase evolution of lead oxide compounds corresponding with oxygen release and absorption processes of BSCCO powders during heat treatment. Superconductor Science and Technology, 2004, 17, 249-255.	3.5	13
126	Effect of post-annealing on critical current density of (Bi,Pb)-2223/Ag tapes. Physica C: Superconductivity and Its Applications, 2004, 412-414, 1091-1095.	1.2	5

#	Article	IF	CITATIONS
127	The stability range of lead oxide compounds in BSCCO-2223 precursor powders. Physica C: Superconductivity and Its Applications, 2004, 407, 115-120.	1.2	1
128	The stability range of lead oxide compounds in BSCCO-2223 precursor powders. Physica C: Superconductivity and Its Applications, 2004, 411, 35-40.	1.2	5
129	Frequency dependence of ac susceptibility of monofilament Bi-2223/Ag superconducting tapes. Physica C: Superconductivity and Its Applications, 2004, 412-414, 1154-1157.	1.2	10
130	Microstructural evolution of Bi-2223/Ag tapes during the cooling process after the first heat treatment. Superconductor Science and Technology, 2003, 16, 1162-1166.	3.5	10